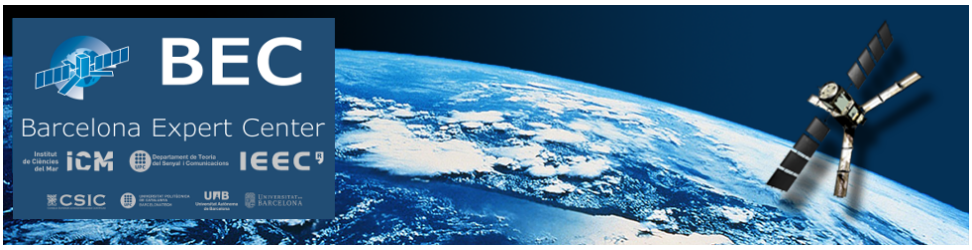

File: BEC-SMOS-0002-PD-NonBayesianSSS.pdf , version 1.0

Title: Global SMOS-BEC Debiased non-Bayesian SSS L3 and L4 Product Description.

Authors: BEC Team.

Contact: smos-bec@icm.csic.es

Date: 15/07/2019

GLOBAL SMOS-BEC DEBIASED NON-BAYESIAN SSS L3 AND L4 PRODUCT DESCRIPTION

Abstract: This technical note describes the retrieval of L3 and L4 SMOS SSS produced and distributed by the BEC team through its data visualization and distribution service http://bec.cmima.csic.es

Contents

1 INTRODUCTION

This is the product specification document for the L3 and L4 SMOS Sea Surface Salinity produced and distributed at BEC.

SMOS-BEC SSS products are generated following a debiased non-Bayesian approach presented in [Olmedo et al., 2017]. The main difference with respect to the standard SSS retrieval is the filtering strategy. In the non-Bayesian approach the filtering strategy is based on the quality of the individual Brightness Temperatures (TB).

2 SCIENCE ALGORITHM OVERVIEW

2.1 Level 2 Algorithms

The debiased non-Bayesian retrieval of SSS introduced in [Olmedo et al., 2017] aims to correct two known issues: the systematic biases caused by the presence of land masses and radio interference, and the data gaps due to the non-convergence of the retrieval algorithm.

2.1.1 Input data

The Brightness temperatures (TBs) obtained from SMOS MIRAS L1B TBs v620 provided by ESA are used as an input for the SMOS SSS retrieval. The L1B v620 product contains the Fourier coefficients of the measured brightness temperature. Starting from this product, using ESA's Earth Observation Customer Furnished Item (EOCFI) orbit propagation libraries [ESA, 2014] and following a similar procedure as the one used in the operational SMOS level 1 processor chain [Deimos, 2014], the measured TBs are obtained in the antenna reference frame (ARF). The unique difference from the standard processor is the number of points contained per snapshot (*i.e.* the resolution). The operational processor uses, at antenna level, a hexagonal grid of 128×128 points (*i.e.* $2^7 \times 2^7$). The projection of this antenna grid into the ground provides a resolution of about 15 km at bore-sight. This resolution is more than twice SMOS theoretical finer resolution [McMullan et al., 2008]. We have thus reduced the computational cost without actually losing information by using an antenna hexagonal grid of 64×64 ($2^6 \times 2^6$) points.

2.1.2 Forward Model

The forward model linking the modeled TB to SSS relies on the dielectric constant model proposed by Klein and Swift [Klein and Swift, 1977] which non-linearly depends on SSS and SST. Nevertheless, the measured TB not only contains information about brightness temperature of the flat sea, but also contributions due to other main sources: the roughness of the sea surface [Guimbard et al., 2012], the reflected emission of the atmosphere, the reflection on the sea surface of the galactic emission ([Tenerelli et al., 2008]) and the sun glitter [Reul et al., 2007]. Therefore, all these additional contributions to the TB(hj, SSS, p1, . . . , pNp) term must be modeled at the bottom of the atmosphere (BOA) and then translated to the ARF prior to minimizing Eq. (1). Thus, the atmospheric attenuation effect over brightness temperature must be taken into account together with the direct emission of the atmosphere itself to estimate the modeled TB at the top of the atmosphere (TOA). Finally, to go from TOA to ARF, the ionosphere must be taken into account. The ionospheric effect translates into a rotation in the polarization components of TB. All these contributions are described in detail in Ocean SMOS Team (2016).

2.1.3 Non-Bayesian retrieval of SSS

We retrieve a single SSS value for each TB measurement, that is, along the same dwell line we have a value of SSS for each valid incidence angle, namely:

$$F^{j}_{non-Bayesian}(SSS) = \left[I^{meas}(\theta_j) - I(\theta_j, SSS, p_1, \ldots, p_{N_p})\right]^2, \quad (1)$$

where the super index j indicates one of the N_m available incidence angles. The term $I = (TB_v + TB_h)/2$, both for the forward modeled (section 2.1.2) and measured data, is the First Stokes parameter at BOA divided by 2; by summing up vertical (TB_v) and horizontal (TB_h) polarization we obtain a

term which is independent from Faraday rotation and simplifies its processing, although the retrieval could be done with each polarization independently. For the optimization, the other geophysical variables are given a fixed value, that of the geophysical priors p_k^0.

2.1.4 SSS spatial bias characterization: definition of a SMOS-based climatology

The characterization of bias is based on a classification of the non-Bayesian single-angle salinities retrieved using eq. (1). A first geophysical consistency filter on non-Bayesian salinities is applied: we discard any value out of the range $[0, 50]$. Then, the single-angle SSS values are grouped together according to their geolocation (latitude and longitude in a cylindrical grid of $0.25^o \times 0.25^o$, φ and λ), overpass direction (ascending or descending, denoted by a binary variable d), across-track distance to the center of swath (in 50-km bins, denoted by x) and incidence angle (in 5° bins, denoted by θ). For each given 5-tuple, $c = (\varphi, \lambda, d, x, \theta)$, we take all the retrievals $\{SSS(\varphi, \lambda, d, x, \theta)\}$ in the period we use (2011 to 2016) and construct the associated histograms (see Figure 1). The choice of the parameters used in the definiton of the tuple is further detailed in [Olmedo et al., 2017] (section 2.2.2).

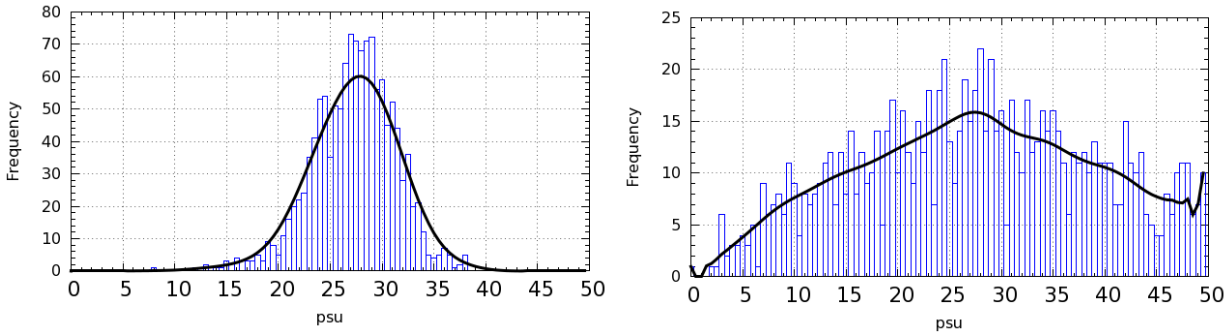

Figure 1: SMOS SSS histogram associated with $c = (20, -29, A, 225, 52)$ (left) and to $c = (31, 133, A, 275, 47)$ (right) (see the text for more details).

For every tuple, the corresponding SSS histogram is defined with bins of 0.5 psu. In order to improve the accuracy of the histogram and minimize the dependency on the histogram discretization, the mean of SSS inside each bin is considered as the representative value of SSS on that bin. The mode of the histograms are taken as a measure of the central reference value; the advantage of taking the mode, instead of other statistics, is that the mode is unaffected by the presence of outliers or by the skewness of the distribution.

The accuracy of the estimation of the mode of any histogram is relatively low, mainly because of the lack of sampling. To overcome this issue we have applied three times a weighted averaging window (with a size of seven points, including the central point, the three points to its left and the three points to its right) to each histogram to eliminate statistically non-significant fluctuations. As shown in Figure 1 (black line), this leads to a better determination of the location of the maximum probability (i.e., the mode). The resulting smoothed histogram is only used for estimating the mode; the rest of statistical parameters are computed from the original (not-smoothed) histogram. We compute a SMOS-based climatological value for each given 5-tuple (denoted as $sss\_clim(\varphi, \lambda, d, x, \theta)$) by averaging all the retrieved single-angle SSSs lying in a range of $\pm\sigma$ around the estimated mode, where σ is the standard deviation of the single-angle SSSs for that 5-tuple.

Figure 2 shows two maps of the SMOS-based climatologies, corresponding to ascending overpasses, $x = 0$ km, $\theta = 5°$ (top) and $\theta = 35°$ (bottom). Significant differences are found for different θ values (that is, depending on the relative position of the pixel in the ARF), see Figure 3. The differences are

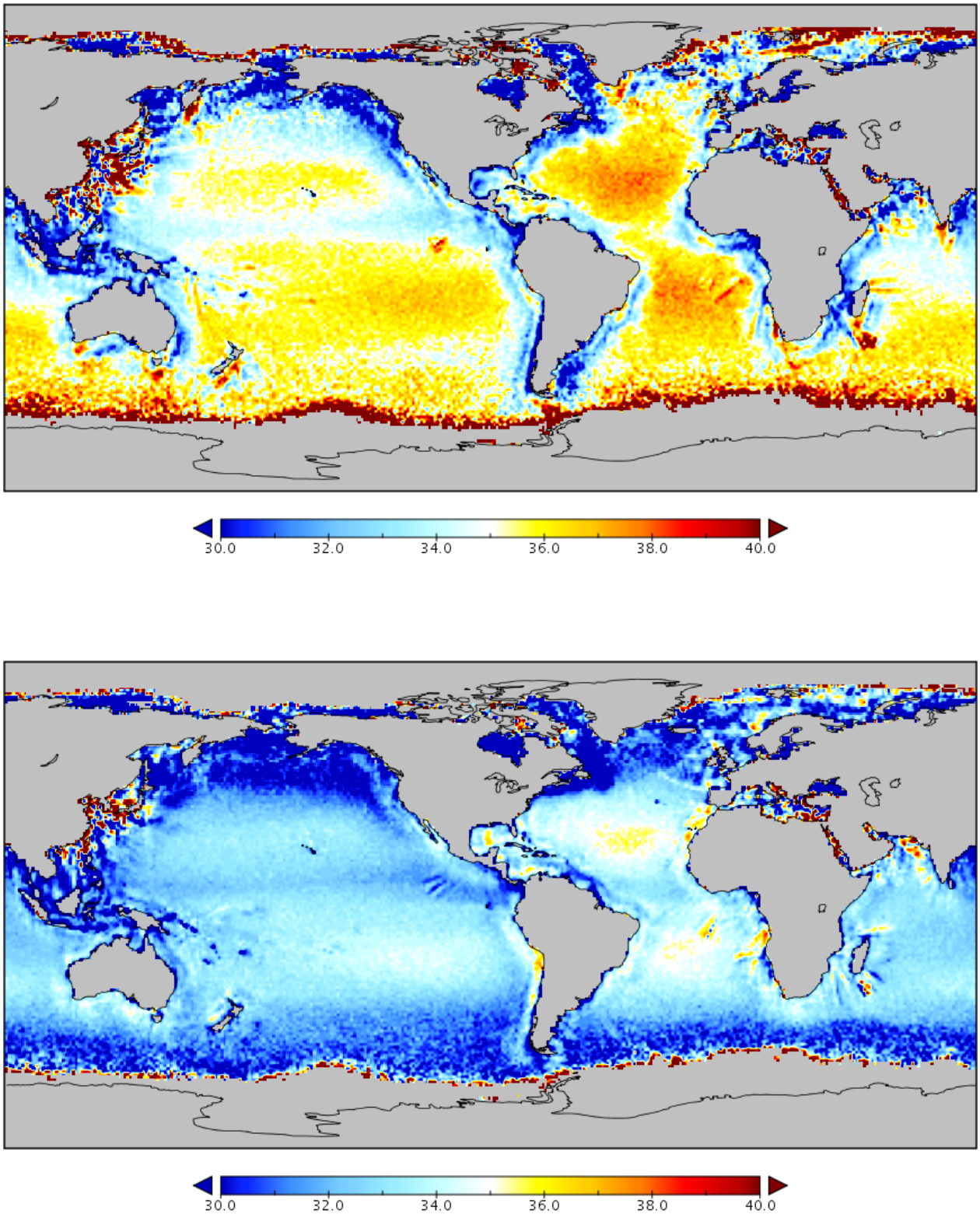

Figure 2: SMOS-based climatology for ascending overpasses and $x = 0$ km and $\theta = 5°$ (top) and $x = 0$ km and $\theta = 35°$ (bottom).

notably large close to the coast due to LSC, although they can be significant also elsewhere. A close inspection of the SMOS-based climatologies shows that for any given value of x and θ the deviation of SMOS-based climatology from a standard annual climatology is far from being spatially constant, even in open sea (see Figure 4).

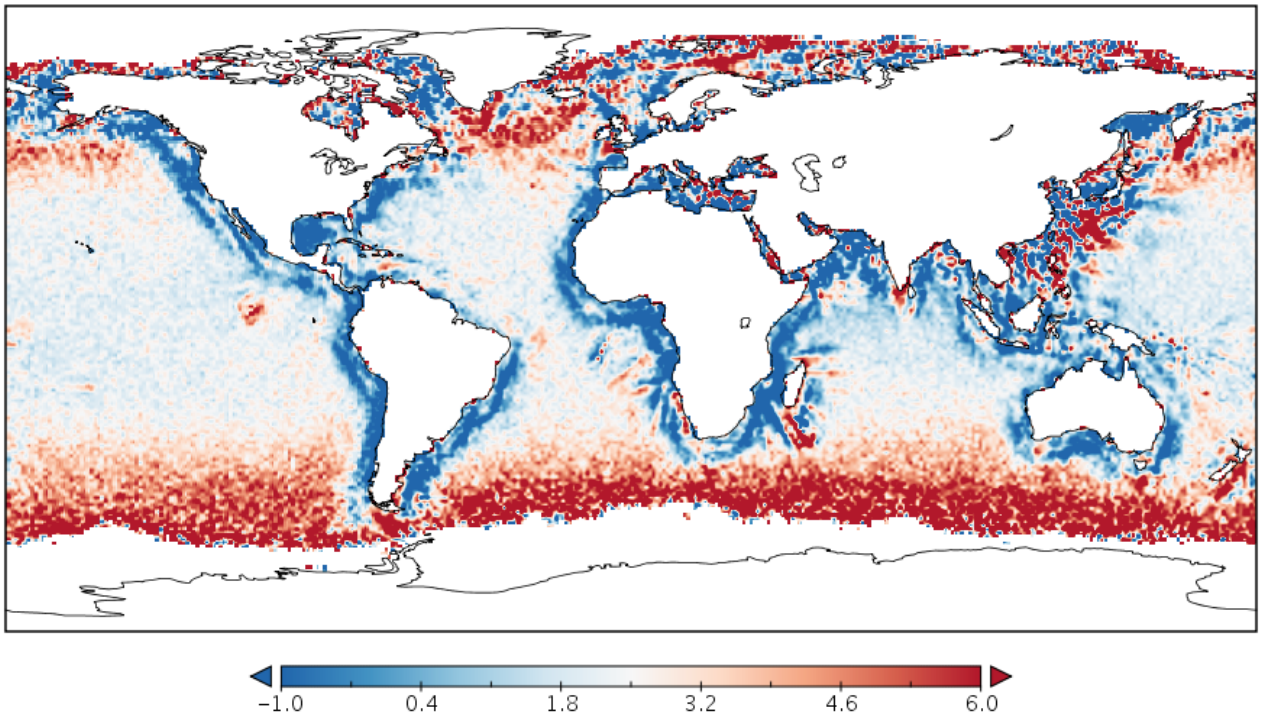

Figure 3: Map of differences between the SMOS-based climatology for ascending overpasses and x=0 km and $\theta = 5^o$ and the SMOS-based climatology for ascending overpasses and x=0 km and $\theta = 35^o$.

2.1.5 Spatial bias correction

For the generation of higher-level SSS products, single-angle SSS retrievals (Section 2) are corrected with their corresponding SMOS-based climatological value (sss_{clim}), thus creating a set of so-called SMOS-based anomalies (sss_{an}):

$$sss_{an}(\varphi, \lambda, d, x, \theta) = SSS(\varphi, \lambda, d, x, \theta) - sss_{clim}(\varphi, \lambda, d, x, \theta). \quad (2)$$

In order to obtain an absolute value of SSS, a time-independent reference SSS value must be added to the L2 product. We use here the annual SSS climatology provided by the World Ocean Atlas 2013 (WOA2013) at $0.25^o \times 0.25^o$ (average decadal product, which is accessible at [National Oceanographic Data Center, [Zweng et al., 2013]).

2.1.6 SSS filtering criteria for non-Bayesian approach

After computing SMOS-based climatologies, several quality control criteria are applied to discard poor quality values. For a given 5-tuple, $c = (\varphi, \lambda, d, x, \theta)$, a SMOS-climatological value is discarded (and

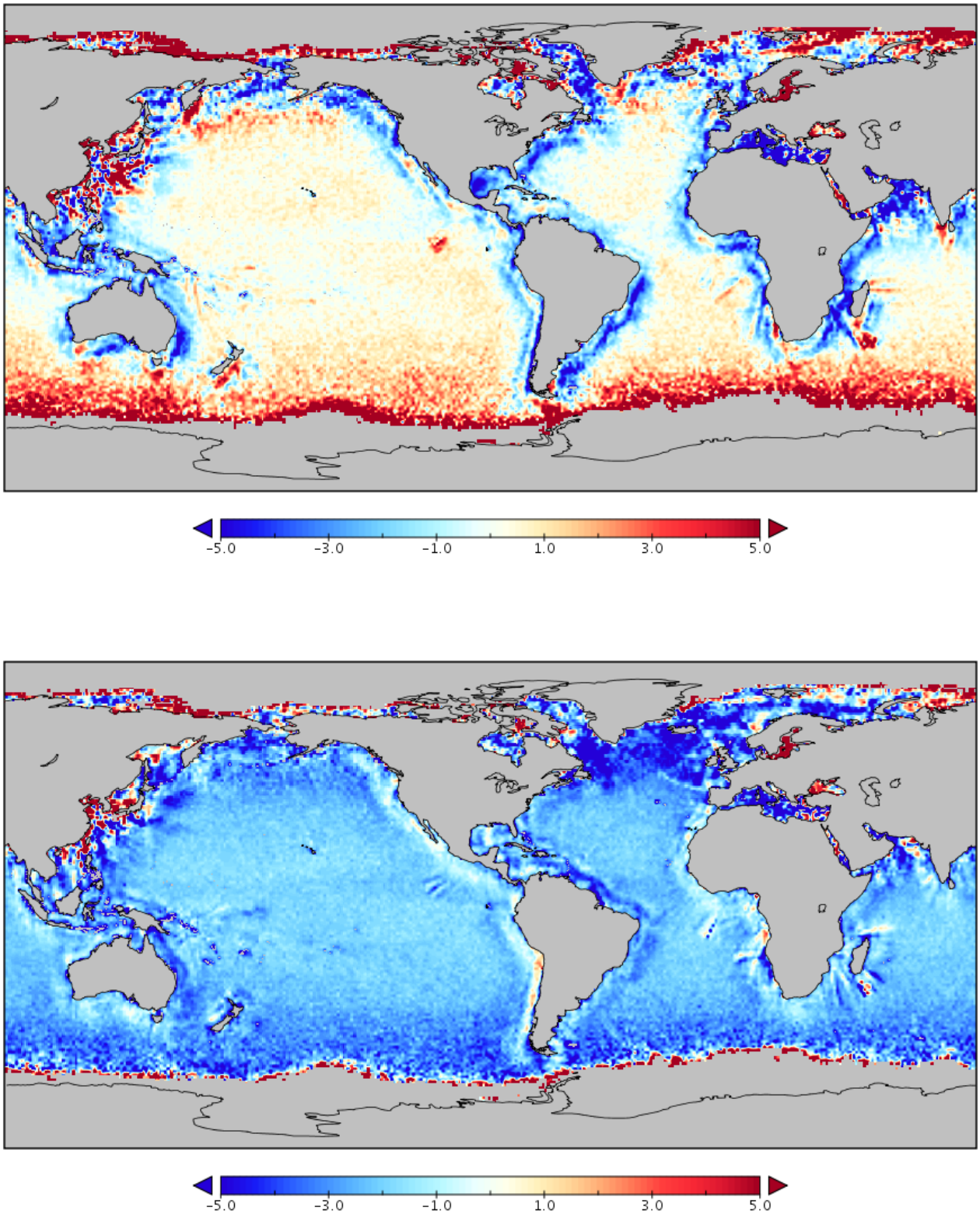

Figure 4: Difference between SMOS-based climatology and the annual WOA2013 climatology for ascending overpasses and $x = 0$ km and $\theta = 5°$ (top) and $x = 0$ km and $\theta = 35°$ (bottom).

hence all related single-angle SSS retrievals) when the associated histogram suffers from one or more of the following conditions:

- It has less than 100 measurements;
- Its standard deviation is greater than 10 psu;
- The absolute value of its normalized skewness is greater than 1;
- Its kurtosis is lower than 2

Two additional filtering criteria are applied to the SMOS-based anomalies:

- If the histogram corresponding to a given geographical and orbital coordinates $c = (\varphi, \lambda, d, x, \theta)$ has been discarded following the criteria of Section 2.1.6, then all the $sss_{an}(\varphi, \lambda, d, x, \theta)$ are also discarded.
- When the SMOS-based anomaly is greater than the standard deviation of the distribution, the value is considered an outlier and, therefore, it is also discarded.

As an example, see the two histograms displayed in Figure 1. The one in the left is accepted, as none of the conditions above is verified (it has 581 measurements, a standard deviation of 2.31, skewness equal to 0.97 and kurtosis equal to 3.74). The one in the right has 369 measurements, a standard deviation 5.82 and a 0.19 skewness, which are right, but its kurtosis (1.79) is too low and, therefore, it is discarded.

2.1.7 Temporal bias mitigation

The temporal bias correction is based on imposing that the SMOS-based anomaly L3 maps (generated for a given time period T) have zero mean over the global ocean.

Then, the global L3 SSS map is corrected by subtracting the mean of the SMOS-based anomalies on the global ocean, in the following way.

$$SSS^T_{corr.an}(\varphi, \lambda) = SSS^T_{an}(\varphi, \lambda) - M^T \tag{3}$$

where M^T is the average anomaly on the global ocean for the period T, namely:

$$M^T = \frac{\Sigma_{\text{valid}\varphi,\lambda} SST^T_{an}(\varphi, \lambda)}{N^T} \tag{4}$$

with N^T the number of grid points with valid φ, λ during T.

From the physical point of view, this correction (i.e., requiring the cancellation of the spatial average of the SSS anomaly on a given region) is equivalent to assume that the amount of salt at surface layer does not change with time in the global ocean.

2.2 L3 Algorithm

L3 SSS maps are generated by means of an objective analysis method, as presented in [Zweng et al., 2013]. The time period has been selected equal to 9 days because it corresponds to a half almost repeat sub-cycle of SMOS, and so it is the shortest time period providing a complete spatial coverage of all the regions. The correlation radii considered are 175, 125 and 75 km.

2.3 L4 Algorithm

L4 SSS maps are obtained with a singularity analysis based fusion technique. The multifractal fusion is a non-parametric technique that merges remotely-sensed maps of different variables to produce higher quality remote sensing products. A higher-quality map of a second ocean variable (Sea Surface Temperature (SST) in our case) is used as a template to restore the multifractal structure of singularity fronts in a noisy variable (SSS in our case). Furter information on the multifractal structure of ocean scalars can be found in [Turiel et al., 2009, Umbert et al., 2014, Olmedo et al., 2016].

Singularity analysis based fusion can be used not only to improve the signal level, but also to increase the spatial and time resolution of fused maps, provided that the template (SST for us) has a better space and time resolutions. Assuming that both variables have the same singularity exponent and we impose the following local relationship:

$$SSS = a \times SST + b \tag{5}$$

where a and b are known as the local slope and intercept coefficients respectively and have small gradients.

The Operational Sea Surface Temperature and Sea Ice Analysis (OSTIA) daily maps at $0.05^o \times 0.05^o$ (see [Donlon et al., 2012]) have been used as a template to increase the spatial and temporal resolution of the 9-day objective analyzed maps. The image averaging used to generate SMOS L3 maps cannot be substantially reduced to less than 9 days because this would result in large data gaps and in an increase of the noise level (at those points with a single or few L2 acquisitions). Therefore, we have used as a signal to be improved L3 9-day SSS maps, generated daily, taking as reference the center of the 9-day period.

3 GLOBAL SSS PRODUCTS

- L3 maps: The product contains the objective analyzed SSS in the corresponding 9-day period at each $0.25^o \times 0.25^o$ cell, and it is daily generated.
- Daily fused L4 maps: The product contains the fused SSS field obtained from the 9-day objective analyzed SSS and the daily OSTIA SST at $0.05^o \times 0.05^o$ grid.

3.1 Ocean files structure

The resulting Level 3 and Level 4 products are distributed in netCDF format and the name of each file follows the layout:

```
BEC_AAAAAA_B_CCCCCCCCCCCCCCC_DDDDDDDDDDDDDDD_EEEEEEE_FFF_GGG.nc
```

Where each field of the filename is as follows:

- AAAAAA: is the product's name:
  - BINNED: Binned product
  - OI____: Optimal Interpolation product

  - L4_SST: Fused product using singularity analysis techniques derived from SST
  - ADVAOA: Advanced?? L3
  - ADVAL4: Advanced?? L4

- B: Indicates the orbit composition of the product.
  - A for products composed by ascending orbits
  - D for products composed by descending orbits
  - B for products composed by both types of orbits
- CCCCCCCCCCCCCCC: Starting UTC time (YYYYMMDDThhmmss) of the first L2 product used to create the L3/L4 product. This is an inherited value in products not derived directly from Level 2 orbits.
- DDDDDDDDDDDDDDD: Ending UTC time (YYYYMMDDThhmmss) of the last L2 product used to create the L3/L4 product. This is an inherited value in products not derived directly from Level 2 orbits (Optimal Interpolation and L4 products).
- FFF: Grid size of the product in a lat-lon grid multiplied by 100
- GGG: Version number of the file starting at 001

3.2 Data Definition

The structure of the netCDF files with its dimensions, variables and global attributes is detailed here:

3.2.1 L3

```
 dimensions:
     lat = 1400 ;
     lon = 720 ;
     time = UNLIMITED ; // (1 currently)
variables:
     float lat(lat) ;
        lat:standard_name = "latitude" ;
        lat:long_name = "Latitude" ;
        lat:units = "degrees_north" ;
        lon:axis = "Y" ;
     float lon(lon) ;
        lon:standard_name = "longitude" ;
        lon:units = "degrees_east" ;
        lon:long_name = "longitude" ;
        lon:axis = "X" ;
     int WGS84 ;
        WGS84:grid_mapping_name = "World Geodetic System 84" ;
        WGS84:longitude_of_prime_meridian = 0.f ;
        WGS84:semi_major_axis = 6378137.f ;
        WGS84:inverse_flattening = 298.2572f ;
     float oa_sss(time, lat, lon) ;
        oa_sss:standard_name = "objective_analyzed_sea_surface_salinity" ;
```

```
        oa_sss:long_name = "Objective Analyzed Sea Surface Salinity" ;
        oa_sss:units = "psu" ;
        oa_sss:description = "Objective analyzed sea surface salinity retrieved from SMOS
measurements" ;
        oa_sss:missing_value = -999.f ;
        oa_sss:_FillValue = -999.f ;
     float std_sss(time, lat, lon) ;
        std_sss:standard_name = "standard_deviation_sea_surface_salinity" ;
        std_sss:long_name = "Standard deviation of the Sea Surface Salinity" ;
        std_sss:units = "psu" ;
        std_sss:description = "Standard deviation of the L2 salinities of each grid point"
;
        std_sss:missing_value = -999.f ;
        std_sss:_FillValue = -999.f ;
     float totalmeasures(time, lat, lon) ;
        totalmeasures:standard_name = "totalmeasures" ;
        totalmeasures:long_name = "Total measures" ;
        totalmeasures:description = "Total L2 salinities measurements of each SMOS grid
point." ;
     float usedmeasures(time, lat, lon) ;
        usedmeasures:standard_name = "usedmeasures" ;
        usedmeasures:long_name = "Used measures" ;
        usedmeasures:description = "Number of measures used for the computation of the
objective analized salinity value" ;
     float uncorrected_binned(time, lat, lon) ;
        uncorrected_binned:standard_name = "uncorrected_binned" ;
        uncorrected_binned:long_name = "Uncorrected intermediate product" ;
        uncorrected_binned:units = "psu" ;
        uncorrected_binned:description = "SSS intermediate data obtained during the non-Bayesi
retrieval.  These data are not included in BEC quality reports.  Not suitable for oceanographi
aplications, for data processing control only" ;
     int time(time) ;
        time:standard_name = "time" ;
        time:long_name = "time" ;
        time:units = "seconds since 1970-1-1 00:00:00" ;
        time:time = "t" ;
        time:coordinate_defines = "center" ;
        time:calendar = "gregorian" ;
        time:_CoordianteAxisType = "Time" ;
global attributes:
     :title = "Objective Analyzed Salinity file" ;
     :genOA_version = "0.1" ;
     :date_created = "2017-03-28 01:37:35 GMT" ;
     :time_coverage_start = "2016-12-31T00:00:00" ;
     :time_coverage_end = "2017-01-09T00:00:00" ;
     :geospatial_lon_units = "degrees_east" ;
     :geospatial_lat_units = "degrees_north" ;
     :geospatial_lon_min = -179.875f ;
     :geospatial_lon_max = 179.875f ;
```

```
     :geospatial_lat_min = -89.875f ;
     :geospatial_lat_max = 89.875f ;
     :institution = "SMOS Barcelona Expert Centre, ICM-CSIC / UPC, Barcelona, Spain" ;
     :copyright = "BEC research products are freely distributed.  SSS have been computed
by means of the algorithm described in Olmedo, E. et al., De-biased non-Bayesian Retrieval:
a novel approach to SMOS Sea Surface Salinity, Remote Sensing of Environment 193 (2017)
103-126.  If these data are used for publication, the following ackowlegment should be
included:  These data were produced by the Barcelona Expert Centre (http://cp34-bec.cmima.csic
a joint initiative of the Spanish Research Council (CSIC) and Technical (University of
Catalonia (UPC), mainly founded by the Spanish National Program on Space" ;
     :references = "Olmedo, E. et al., De-biased non-Bayesian Retrieval:  a novel approach
to SMOS Sea Surface Salinity, Remote Sensing of Environment 193 (2017) 103-126." ;
     :Conventions = "CF-1.4" ;
```

3.2.2 L4

```
 dimensions:
     lat = 3600 ;
     lon = 7200 ;
     time = UNLIMITED ; // (1 currently)
variables:
     float lat(lat) ;
        lat:standard_name = "latitude" ;
        lat:long_name = "Latitude" ;
        lat:units = "degrees_north" ;
        lon:axis = "Y" ;
     float lon(lon) ;
        lon:standard_name = "longitude" ;
        lon:units = "degrees_east" ;
        lon:long_name = "longitude" ;
        lon:axis = "X" ;
     float l4_sss(time, lat, lon) ;
        l4_sss:standard_name = "l4_sea_surface_salinity" ;
        l4_sss:long_name = "L4 Sea Surface Salinity" ;
        l4_sss:units = "psu" ;
        l4_sss:description = "Sea Surface Salinity analysis using Data Fusion of SST"
;
        l4_sss:missing_value = -999.f ;
        l4_sss:_FillValue = -999.f ;
     float quality_flag(time, lat, lon) ;
        quality_flag:standard_name = "quality_flag" ;
        quality_flag:long_name = "Quality control flag" ;
        quality_flag:units = "-" ;
        quality_flag:description = "When the flag is equal to 1 the corresponding value
of salinity has been extrapolated." ;
        l4_sss:missing_value = -1 ;
        l4_sss:_FillValue = -1 ;
     int time(time) ;
```

```
        time:standard_name = "time" ;
        time:long_name = "time" ;
        time:units = "seconds since 1970-1-1 00:00:00" ;
        time:time = "t" ;
        time:coordinate_defines = "center" ;
        time:calendar = "gregorian" ;
        time:_CoordianteAxisType = "Time" ;
global attributes:
     :title = "Sea Surface Salinity L4 map" ;
     :date_created = "2017-03-30 02:22:25 +0200 UTC" ;
     :time_coverage_start = "2011-03-14T00:00:00" ;
     :time_coverage_end = "2011-03-14T59:59:59" ;
     :geospatial_lon_units = "degrees_east" ;
     :geospatial_lat_units = "degrees_north" ;
     :geospatial_lon_min = -179.875f ;
     :geospatial_lon_max = 179.875f ;
     :geospatial_lat_min = -89.875f ;
     :geospatial_lat_max = 89.875f ;
     :institution = "SMOS Barcelona Expert Centre, ICM-CSIC / UPC, Barcelona, Spain" ;
     :copyright = "BEC research products are freely distributed.  SSS have been retrieved
following the algorithm described in Olmedo, E. et al., Debiased non-Bayesian Retrieval:
a novel approach to SMOS Sea Surface Salinity, Remote Sensing of Environment 193 (2017)
103-126, and fusion with SST has been computed following the algorithm described in Olmedo,
E. et al., Improving time and space resolution of SMOS salinity maps using multifractal
fusion, Remote Sensing of Environment 180 (2016) 246-263.  If these data are used for
publication, the following ackowlegment should be included:  These data were produced
by the Barcelona Expert Centre (http://cp34-bec.cmima.csic.es), a joint initiative of
the Spanish Research Council (CSIC) and Technical (University of Catalonia (UPC), mainly
founded by the Spanish National Program on Space" ;
     :references = "Olmedo, E. et al., De-biased non-Bayesian Retrieval:  a novel approach
to SMOS Sea Surface Salinity, Remote Sensing of Environment 193 (2017) 103-126.  and Olmedo,
E. et al., Improving time and space resolution of SMOS salinitymaps using multifractal
fusion, Remote Sensing of Environment 180 (2016) 246-263" ;
     :Conventions = "CF-1.4" ;
```

3.3 Data Access

The Global SMOS SSS v1.0 produced at BEC is freely available through a SFTP server. If your browser is SFTP compatible you can browse directly from sftp://becftp.icm.csic.es:27500 address. The data can be download after completing registration in our BEC ftp service (http://bec.icm.csic.es/bec-ftp-service-registration/). For more information about the BEC ftp service, please visit http://bec.icm.csic.es/bec-ftp-service/. For any further assistance, contact to smos-bec@icm.csic.es.

The following diagram tree shows the complete path to the Global SMOS SSS v1.0 repository.

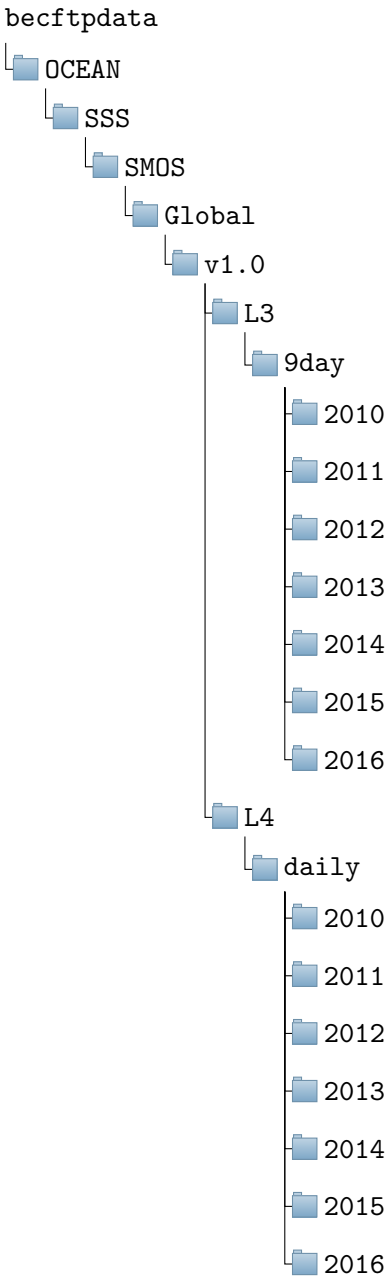
becftpdata
OCEAN
SSS
SMOS
Global
v1.0
L3
9day
2010
2011
2012
2013
2014
2015
2016
L4
daily
2010
2011
2012
2013
2014
2015
2016

A QUALITY ASSESSMENT

The aim of this section is to report the differences between the non-Bayesian debiased L3 (weighted averaged and objective analyzed) and L4 (fused) SMOS SSS distributed by BEC and the Argo data. Table 1 summerizes the nomenclature of the validated products in this section.

Frequency	**Average Period**	**Grid**	**Orbit**	**Product**	**Name**
daily	1 days	$0.05^o \times 0.05^o$	both	Fused	ADVAL4
daily	9 days	$0.25^o \times 0.25^o$	both	Objective Analyzed	ADVAOA
daily	9 days	$0.25^o \times 0.25^o$	both	Weighted averaged	ADVAWA

Table 1: Ocean products validated in this study.

A.1 Argo

The SMOS-BEC products are compared in this section with in situ data. The statistical comparison is carried out with close-to-surface values acquired by Argo floats (Argo float data and metadata from Global Data Assembly Centre (Argo GDAC). SEANOE. http://doi.org/10.17882/42182).

In particular, SSS values are being estimated from Argo the uppermost SSS value. Only profiles with valid values at (at least) 10m depth are considered. For SOLO and PROVOR profiles, only data below 5 m depth are taken into account as their CTD probes do stop pumping water at arround 5 m below the surface. The whole valid profile is used in the interpolation, with the exception of values taken above 0.5 m depth.

The differences between satellite and the external data are estimated in the regions described in table 2.

Zone	**Description**	**Latitude**	**Longitude**
Global	Tropics and mid-latitudes	60^oS - 60^oN	All
Tropic	Tropics	30^oS - 30^oN	All
122	A region of the South Eastern Pacific	30^oS - 0^oN	150^oW - 120^oW
124	A region of the South Western Tropical Pacific	24^oS - 10^oS	165^oE - 165^oW
126	Equatorial oceans	10^oS - 10^oN	All
NPac	North Pacific region	45^oN - 60^oN	170^oE - 140^oW
131	Southern Ocean	60^oS - 40^oS	All
132	Intertropical Pacific	5^oN - 15^oN	110^oW - 180^oW
Ant	Antarctic	90^oS - 50^oS	All
Arc	Arctic	50^oN - 90^oN	All
Med	Mediterranean Sea	30^oN - 47^oN	35^oW - 35^oE

Table 2: Zones under study

The values listed in the table 4 correspond to the global average value of the mean, the standard deviation and the root mean square statistics with respect to the different SMOS SSS procuts during the years 2011 and 2016. A more detailed analysis under the regions described in 2 are presented for each product: weighted averaged, objective analyzed and fused L4 SSS in separate in Tables 5, 6 and 7, respectively. The time evolution of some of these statistics is shown in Figures 5, 6, 7, 8, 9 and 10.

Table 3: Summary of statistics of the comparison with Argo

Product	<Mean>	<STD>	<RMS>
ADVAWA	-0.13	0.42	0.46
ADVAOA	0.01	0.25	0.27
ADVAL4	-0.01	0.21	0.21

Table 4: Statistics of the comparison with Argo

		SMOS - ARGO in [60^{o}S:60^{o}N]			**SMOS - ARGO in [30^{o}S:30^{o}N]**		
Year	Product	<Mean>	<STD>	<RMS>	<Mean>	<STD>	<RMS>
2011	ADVAWA	-0.08	0.41	0.43	-0.05	0.37	0.38
	ADVAOA	0.02	0.24	0.24	0.05	0.23	0.24
	ADVAL4	-0.01	0.21	0.21	0.03	0.22	0.22
2012	ADVAWA	-0.04	0.40	0.41	-0.03	0.37	0.37
	ADVAOA	0.02	0.24	0.24	0.05	0.23	0.24
	ADVAL4	-0.00	0.20	0.20	0.02	0.22	0.22
2013	ADVAWA	-0.08	0.41	0.43	-0.06	0.38	0.40
	ADVAOA	0.01	0.24	0.24	0.05	0.24	0.25
	ADVAL4	-0.01	0.20	0.20	0.01	0.22	0.22
2014	ADVAWA	-0.14	0.42	0.46	-0.12	0.39	0.42
	ADVAOA	0.02	0.25	0.26	0.06	0.25	0.26
	ADVAL4	-0.01	0.22	0.22	0.03	0.24	0.24
2015	ADVAWA	-0.15	0.43	0.46	-0.11	0.39	0.41
	ADVAOA	0.03	0.26	0.26	0.08	0.26	0.28
	ADVAL4	-0.01	0.23	0.23	0.04	0.25	0.26
2016	ADVAWA	-0.17	0.44	0.48	-0.12	0.41	0.43
	ADVAOA	0.01	0.28	0.28	0.08	0.28	0.29
	ADVAL4	-0.02	0.24	0.24	0.05	0.26	0.27

Table 5: Statistics of the comparison with Argo: Weighted Averaged SSS

Region	IQR	Median	Mean	STD	RMS
122	0.41	-0.09	-0.08	0.29	0.33
124	0.45	-0.08	-0.07	0.33	0.36
126	0.53	-0.07	-0.06	0.38	0.41
131	0.65	-0.20	-0.19	0.47	0.53
132	0.48	-0.04	-0.02	0.34	0.39
Tropic	0.53	-0.12	-0.10	0.39	0.42
Global	0.58	-0.15	-0.13	0.42	0.46
Ant	0.78	-0.22	-0.20	0.56	0.62
Arc	0.92	-0.22	-0.20	0.66	0.72
Med	1.06	-0.35	-0.31	0.76	0.85
NPac	0.84	-0.20	-0.18	0.60	0.67

Table 6: Statistics of the comparison with Argo: Objective Analyzed SSS

Region	IQR	Median	Mean	STD	RMS
122	0.25	0.07	0.08	0.18	0.22
124	0.28	0.07	0.08	0.20	0.24
126	0.38	0.08	0.09	0.28	0.32
131	0.30	-0.07	-0.08	0.22	0.23
132	0.35	0.12	0.13	0.24	0.34
Tropic	0.34	0.03	0.05	0.25	0.27
Global	0.34	-0.01	0.01	0.25	0.27
Ant	0.30	-0.14	-0.14	0.21	0.26
Arc	0.39	-0.15	-0.15	0.28	0.36
Med	0.52	-0.16	-0.18	0.37	0.43
NPac	0.40	-0.10	-0.10	0.28	0.36

Table 7: Statistics of the comparison with Argo: Fused L4 SSS

Region	IQR	Median	Mean	STD	RMS
122	0.22	0.07	0.08	0.16	0.18
124	0.26	0.06	0.08	0.19	0.21
126	0.38	0.08	0.10	0.28	0.30
131	0.18	-0.06	-0.06	0.13	0.15
132	0.36	0.17	0.18	0.25	0.35
Tropic	0.32	0.01	0.03	0.23	0.24
Global	0.29	-0.03	-0.01	0.21	0.21
Ant	0.18	-0.07	-0.07	0.13	0.15
Arc	0.33	-0.19	-0.19	0.23	0.33
Med	0.58	-0.23	-0.28	0.38	0.48
NPac	0.34	-0.11	-0.12	0.24	0.31

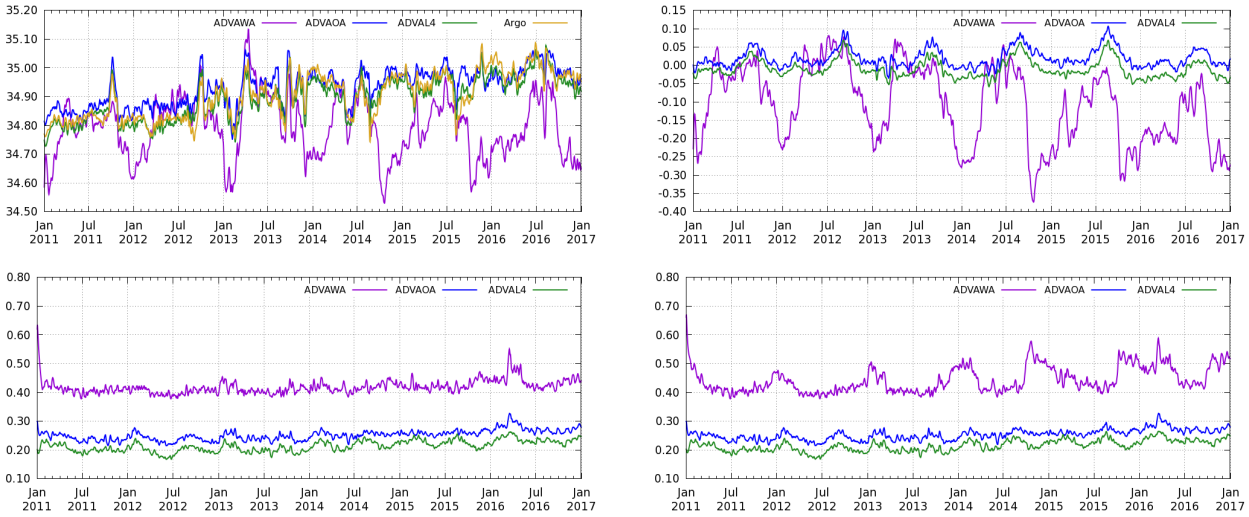

Figure 5: Differences of the SMOS SSS with respect to ARGO in global region: Top left the average of SSS in the colocations; top right the mean of the difference between SMOS and ARGO SSS, bottom left the standard deviation of the difference; bottom right the rms of the difference.

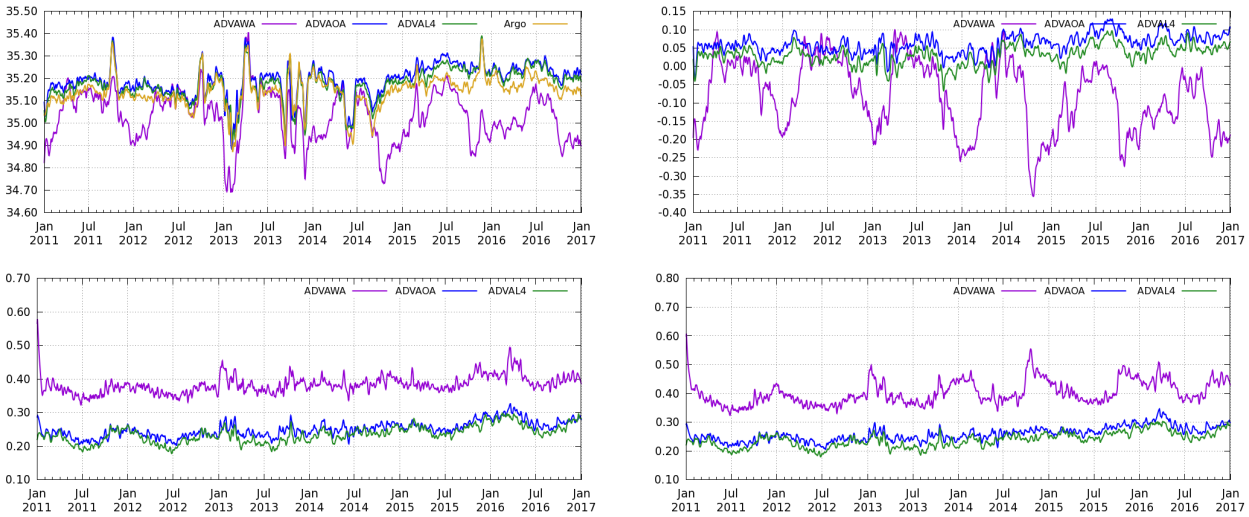

Figure 6: Differences of the SMOS SSS with respect to ARGO in tropical region: Top left the average of SSS in the colocations; top right the mean of the difference between SMOS and ARGO SSS, bottom left the standard deviation of the difference; bottom right the rms of the difference.

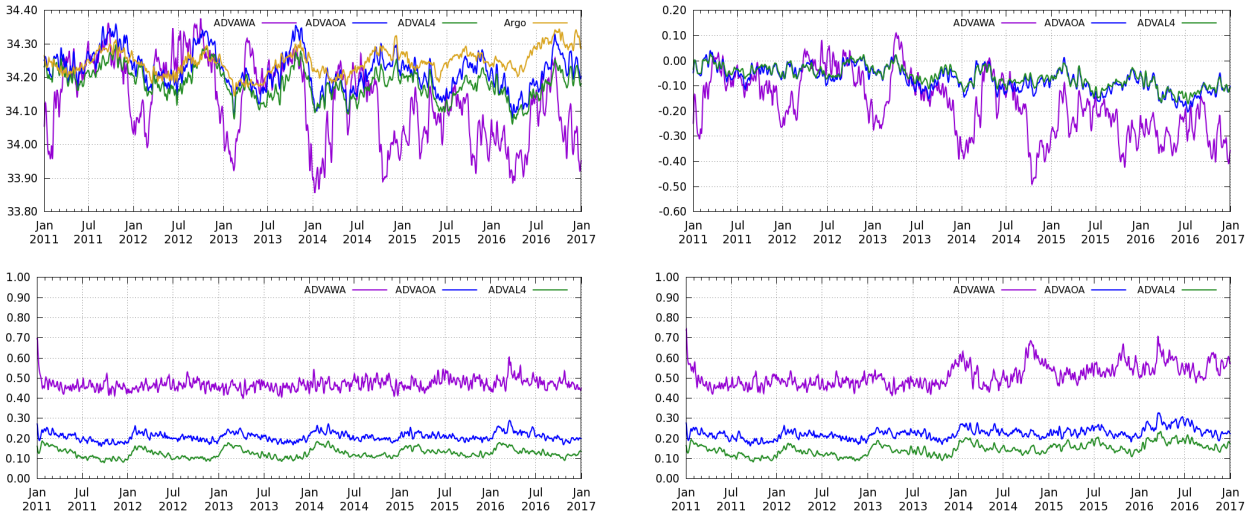

Figure 7: Differences of the SMOS SSS with respect to ARGO in region 131: Top left the average of SSS in the colocations; top right the mean of the difference between SMOS and ARGO SSS, bottom left the standard deviation of the difference; bottom right the rms of the difference.

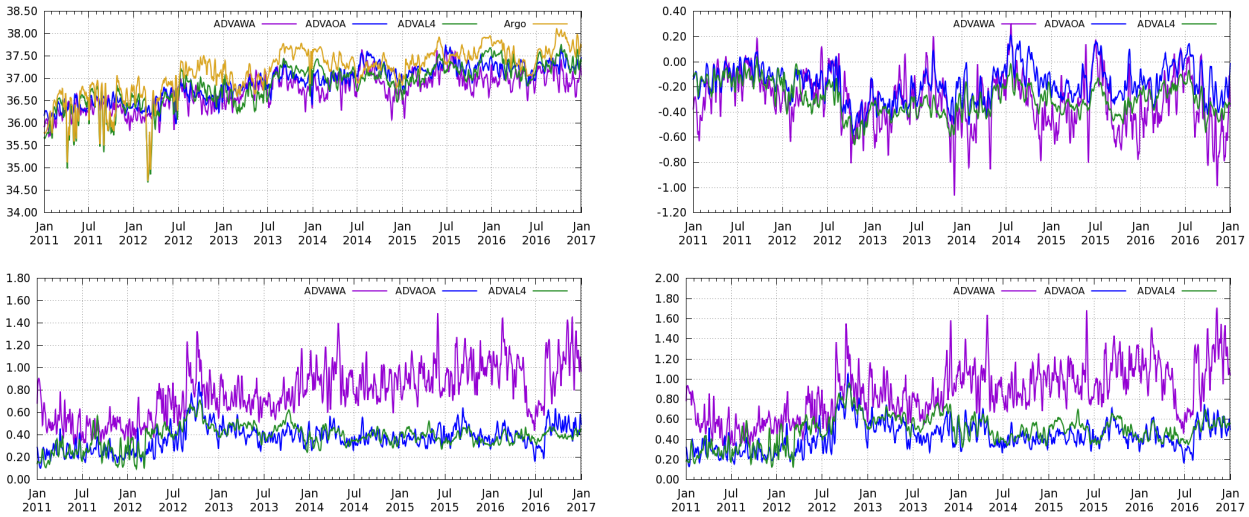

Figure 8: Differences of the SMOS SSS with respect to ARGO in Mediterranean Sea region: Top left the average of SSS in the colocations; top right the mean of the difference between SMOS and ARGO SSS, bottom left the standard deviation of the difference; bottom right the rms of the difference.

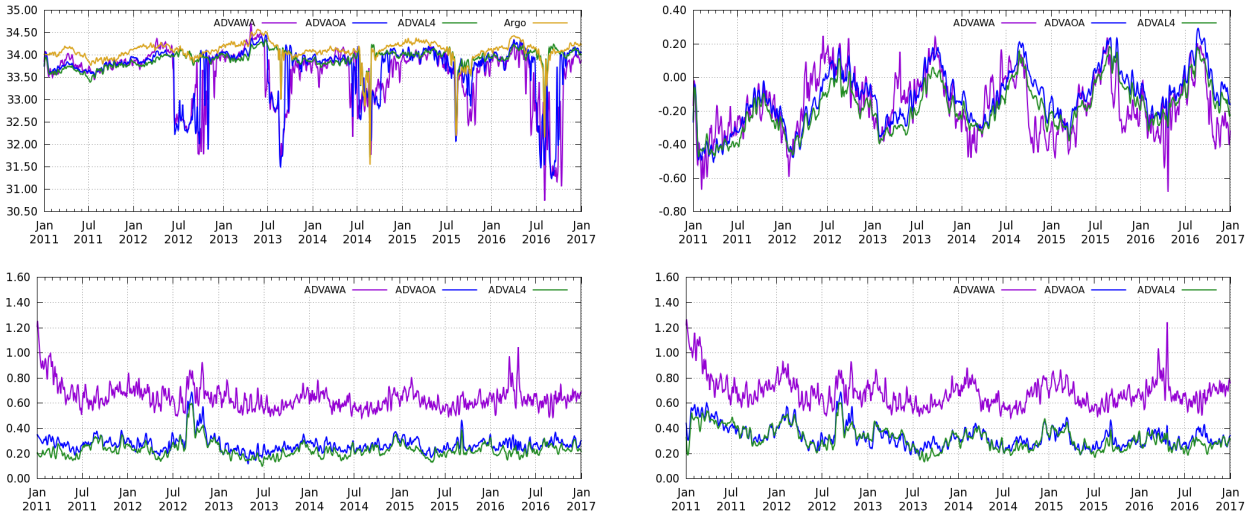

Figure 9: Differences of the SMOS SSS with respect to ARGO in Arctic region: Top left the average of SSS in the colocations; top right the mean of the difference between SMOS and ARGO SSS, bottom left the standard deviation of the difference; bottom right the rms of the difference.

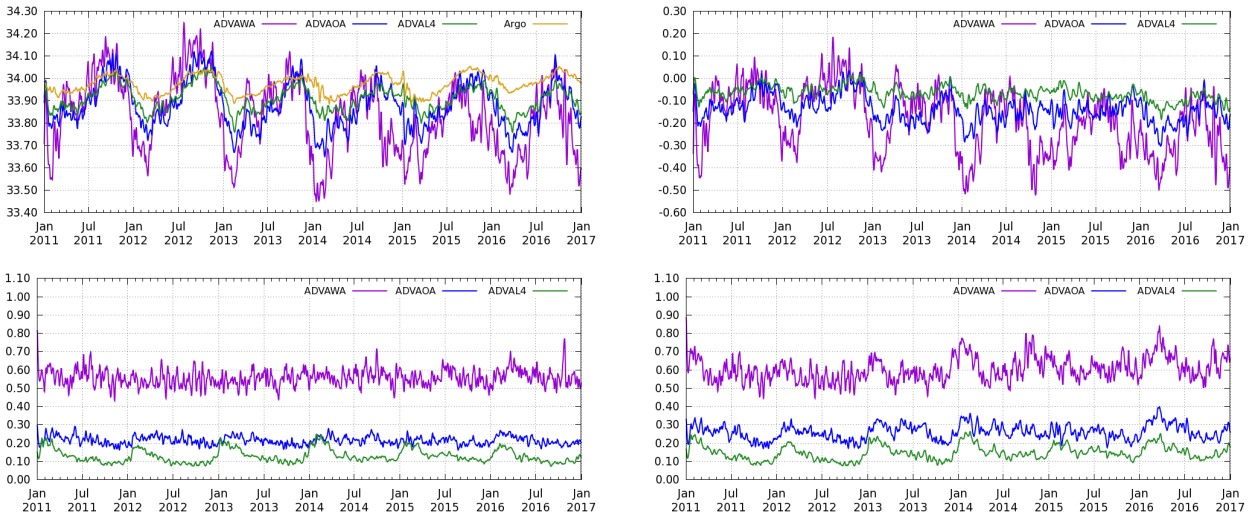

Figure 10: Differences of the SMOS SSS with respect to ARGO in Antartic region: Top left the average of SSS in the colocations; top right the mean of the difference between SMOS and ARGO SSS, bottom left the standard deviation of the difference; bottom right the rms of the difference.

References

[Deimos, 2014] Deimos (2014). *SMOS L1 Processor L1C Data Prorocessing Model. SO-DS-DME-L1PP-0009*. Deimos. version 2.14.

[Donlon et al., 2012] Donlon, C. J., Martin, M., Stark, J., Roberts-Jones, J., Fiedler, E., and Wimmer, W. (2012). The operational sea surface temperature and sea ice analysis (ostia) system. *Remote Sensing and Enviroment*, 116(0):140 – 158.

[ESA, 2014] ESA (2014). Earth Observation CFI v3.x branch. http://eop-cfi.esa.int/index.php/mission-cfi-software/eocfi-software/branch-3-x. [Online; accessed 23-August-2016].

[Guimbard et al., 2012] Guimbard, S., Gourrion, J., Portabella, P., Turiel, A., Gabarró, C., and Font, J. (2012). SMOS Semi-Empirical Ocean Forward Model Adjustement. *IEEE Trans. Geosci. Remote Sens., vol. 50, no. 5. pp. 1676-1687.*

[Klein and Swift, 1977] Klein, L. A. and Swift, C. T. (1977). An improved model for the dialectric constant of sea water at microwave frequencies. *IEEE Trans. on Antennas and Propagation*, 25:104–111.

[McMullan et al., 2008] McMullan, K. D., Brown, M., Martin-Neira, M., Rits, W., Ekholm, S., Marti, J., and Lemanczyk, J. (2008). SMOS: The Payload. *Geoscience and Remote Sensing, IEEE Transactions on*, 46(3):594–605.

[National Oceanographic Data Center, 2013] National Oceanographic Data Center (2013). WOA 2013 V2 Data Access. https://www.nodc.noaa.gov/cgi-bin/OC5/woa13/woa13.pl. [Online; accessed 23-August-2016].

[Olmedo et al., 2016] Olmedo, E., Martínez, J., Umbert, M., Hoareau, N., Portabella, M., Ballabrera-Poy, J., and Turiel, A. (2016). Improving time and space resolution of smos salinity maps using multifractal fusion. *Remote Sensing of Enviroment.*

[Olmedo et al., 2017] Olmedo, E., MartÃnez, J., Turiel, A., Ballabrera-Poy, J., and Portabella, M. (2017). Debiased non-bayesian retrieval: A novel approach to smos sea surface salinity. *Remote Sensing of Environment*, 193:103 – 126.

[Reul et al., 2007] Reul, N., Tenerelli, J., Chapron, B., and Waldteufel, P. (2007). Modeling Sun glitter at L-band for sea surface salinity remote sensing with SMOS. *IEEE Trans. Geosci. Remote Sens.*, 45:2073–2087.

[Tenerelli et al., 2008] Tenerelli, J. E., Reul, N., Mouche, A. A., and Chapron, B. (2008). Earth Viewing L Band Radiometer Sensing of Sea Surface Scattered Celestial Sky Radiation-Part I: General Characteristics. *Geoscience and Remote Sensing, IEEE Transactions on*, 46(3):659–674.

[Turiel et al., 2009] Turiel, A., Nieves, V., García-Ladona, E., Font, J., Rio, M.-H., and Larnicol, G. (2009). The multifractal structure of satellite sea surface temperature maps can be used to obtain global maps of streamlines. *Ocean Science*, 5(4):447–460.

[Umbert et al., 2014] Umbert, M., Hoareau, N. Turiel, A., and Ballabrera-Poy, J. (2014). New blending algorithm to synergize ocean variables: the case of SMOS sea surface salinity maps. *Remote Sensing of Environment 146, pp. 188-200.*

[Zweng et al., 2013] Zweng, M. M., Reagan, J. R., Antonov, J. I., Locarnini, R. A., Mishonov, A. V., Boyer, T. P., Garcia, H. E., Baranova, O. K., Johnson, D. R., Seidov, D., and Biddle, M. M. (2013). *World Ocean Atlas 2013, Volume 2: Salinity.* Levitus, Ed., A. Mishonov Technical Ed.; NOAA Atlas NESDIS 74, 39 pp.